Original
Received August 30, 2001
Accepted for Publication December 18, 2001

Surface Hardening of Some Cast Irons with Inserted Hard Alloy Particles

Kazuhiko OKADA*, Shinya IDETSU*, Shoji GOTO**,
Setsuo ASO** and Yoshinari KOMATSU**

*Automobile Foundry Co., Ltd., 4-2 Kitakandatsu-machi Tsuchiura city 300-0015 Ibaraki prefecture Japan
**Faculty of Engineering and Resource Science, Akita University, 1-1 Tegata Gakuencho Akita city
010-8502 Akita prefecture Japan
E-mail : kazuhiko-okada@jik.iss.co.jp

In this paper, two experiments for locally hard facing of cast iron and cast steel will be presented. In the case of locally hard faced spheroidal graphite cast iron with hard alloy briquettes, the inserted layer as formed with penetration of the molten cast iron among tungsten carbide (henceforth, it is described as WC) particles in the hard alloy briquette. The base metal of inserted layer showed a microstructure of gray cast iron due to a hindrance to spheroidalization caused by a reaction the molten cast iron to the elements of W and Co in the hard alloy. The hardness of mother spheroidal graphite cast iron was about Vickers hardness (henceforth, it is described as HV) 200 while the hardness of the inserted layer ranged from HV600 to HV1600.

In the case of locally hard faced cast steel, the inserted layer was also formed with similar process to that of the spheroidal graphite cast iron, while intermediate phases with very hard complex carbide were formed at the bonding region between the inserted layer and the base metal. The hardness of mother cast steel was about HV300, while the hardness of the inserted layer ranged from HV800 to HV1400. Especially, the intermediate layer with complex carbide showed the highest hardness of HV1800. Therefore, the inserted methods with hard alloy particles are considered to be a very effective one for locally hard facing of cast iron and cast steel.

Key Words : insert, surface hardening, cast iron, cast steel, hard alloy

1. Introduction

Cast iron and cast steel have large degrees of configurational freedom in production of the engineering articles. Since they are cheap, they are widely used as the materials for industrial machineries. However, in order to be adapted for machines in the mining engineering works, it is a drawback that the quality for wear resistance is insufficient. This high abrasiveness is related to a low fracture strength and a low hardness of the materials. These properties have been improved by surface quenching, welding and brazing of hard materials until now. However, these methods have very complicated processes and then require high cost operations, so that they are unsuitable for practical use. Then we have used a method of the insert surface hardening for cast iron and cast steel with the hard alloy particles (WC) to develop the wear resistance.

2. Hard facing of cast iron with hard alloy particles

2.1 Experimental method

The configuration of self-curing mold used in this experiment is shown in Fig. 1. A small amounts of sodium silicate (water glass) was added to the hard alloy powder (WC-6mass%Co, $< 270\,\mu$m) as a binder to make the slurry. The slurry was pasted flat and smoothly by a thickness of 3mm onto the bottom of a test piece as shown in Fig. 1.

The base material used for the cast-in-insert was a spheroidal graphite cast iron which was made from the melt blending a steel scrap, return scrap, graphite powder and Fe-75mass%Si alloy as the raw materials. For the melting, a high frequency induction furnace with a capacity of 100kg was used. Furthermore, the

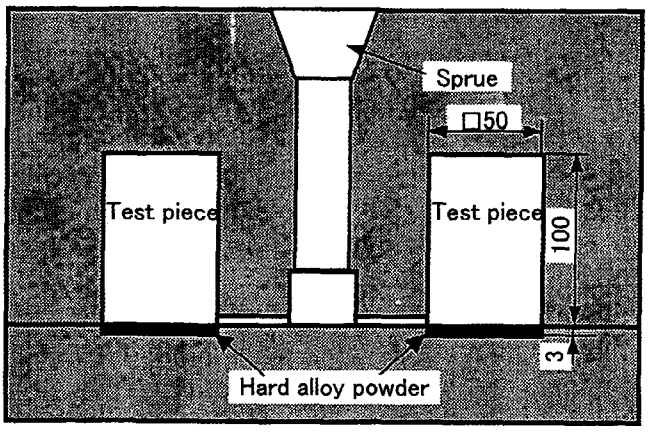

Figure 1 Configuration of mold.

spheroidizing treatment was applied by the sandwich method in which a small amounts of Fe-45mass%Si-4.5mass%Mg alloy was added into the pouring ladle. Composition of the obtained molten iron was C : 3.84, Si : 2.57, Mn : 0.26, S : 0.010, Cr : 0.040, Cu : 0.10 and Mg : 0.046 mass%.

After drying the slurry past layer of the applied hard alloy in the mold sufficiently, the space in the mold was permeated by the molten iron at the temperature of 1693K for conducting the cast-in-insert experiment. The condition for the inserted layer formation was investigated from the points of microstructure and hardness in the obtained test pieces.

2.2 Experimental Result and discussion

2.2.1 Circumstance of Inserted Layer

In order to investigate the configuration of the inserted layer formed under the cast-in-insert conditions, the test piece was cut perpendicular to the bottom surface. And the microstructure of the hard alloy layer on the cut surface was observed by a scanning electron microscope (henceforth, it is described as SEM). An example of results obtained is shown in Fig. 2 as a macro photograph of the cross section. It is observed that the inserted layer of the hard alloy powder is formed in the front surface region of the test piece. The thickness of the inserted hard alloy layer is recognized to be thicker than the initial thickness (the thickness before casting was about 3mm). This phenomenon is thought to be due to the penetration of molten iron among the WC particles in the hard alloy powder to form the alloy-cast-iron layer. That is, the hard alloy layer will expand by a volume of the penetrated molten iron, which will be discussed in detail later. Figure 3 shows the microstructure of the inserted layer. Moreover, Fig. 4 shows the distribution of each element in the neighborhood of a bonding region, which was investigated by electron probe microanalyser (henceforth, it is described as EPMA) image. As seen in Fig. 3, the alloy layer is formed by the penetration of molten iron, so that each hard alloy particle was enclosed by the molten iron. In this case, the morphology of graphite particles in the cast iron is flake-like. This is considered as a result from that spheroidization of graphite is inhibited by elution of W and Co elements of the hard alloy powder into the cast iron matrix. Incidentally, both of the Fe-Co and Fe-W constitutional phase diagrams show a minimum point in the liquidus curve, which is at 1750K for Fe-Co, and 1798K for Fe-W[1] These temperatures are quite close to the pouring temperature of 1693K in this experiment. Therefore, taking into consideration of decreasing of melting point in multi component system such as Fe-C-Si-W-Co system, the elution of W and Co elements from the hard alloy powder during the teeming may be well considered.

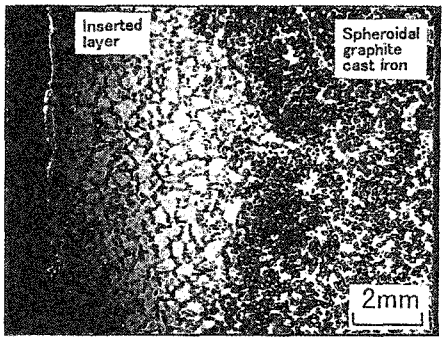

Figure 2 Macrostructure of the vertical section in the inserted test piece. (In case of spheroidal graphite cast iron.)

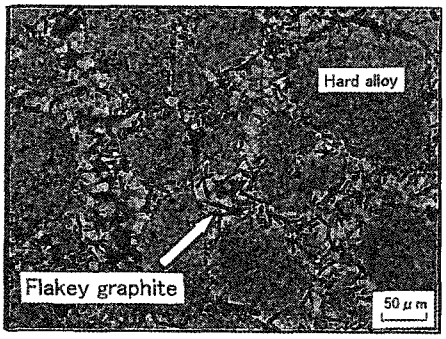

Figure 3 Typical cross-section microstructure of inserted layer.

As seen in Fig. 4, Fe and Si elements have deeply permeated into the hard alloy layer, while Co element has widely distributed in both layers of the inserted layer and the cast iron. Therefore, this fact shows an evidence for fusional diffusion of such elements into the hard alloy powder during the teeming.

2.2.2 Hardness of Inserted Layer

In order to investigate the degree of hard facing by the cast-in-insert method, the hardness distribution in the inserted layer was measured by the micro Vickers hardness test (load ; 2.94N). The results obtained are shown in Fig. 5.

The hardness values in the inserted layer ranged from HV600 to

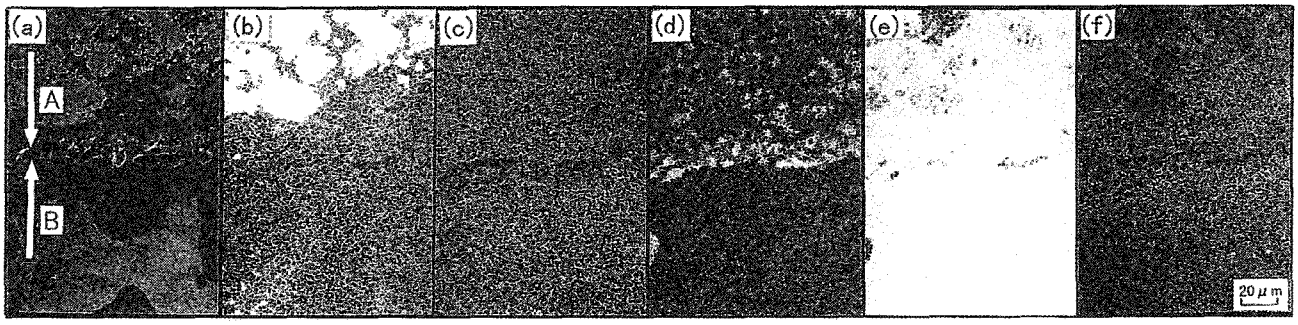

Figure 4 SEM cross-sectional image and EPMA in the insert specimen, which show (a) SEM image, (b) W map, (c) Co map (d) C map, (e) Fe map and (f) Si map.
A and B show the inserted layer and spheroidal graphite cast iron respectively.

1600. These values are sufficiently high in comparison with the hardness of HV200 in the cast iron base metal. Therefore, this cast-in-insert method is concluded to be very effective for the hard facing of spheroidal graphite cast iron material.

By the way, in the bonding region between the inserted layer and the cast iron base material the hardness is decreasing gradually. This is considered to be due to a violent reaction between the hard alloy powder and the cast iron base material. In order to clarify this point, SEM observation and EPMA line-analysis of the hard alloy powder in inserted layer were conducted. The results obtained are shown in Fig. 6 and Fig. 7. The hardness in Fig. 6 and Fig. 7 corresponded to HV1200 and HV600, respectively.

In the case of HV1200 (Fig. 6) interparticle spacing of WC particles in the hard alloy powder is much smaller in the central part than in the outer rim region, in which the particle number density of WC is also lower. Moreover, it is observed that concentration of Co element is much higher in the central part than in the outer rim region. On the other hand, in the case of HV600 (Fig. 7) the inter particle spacing of WC particles is much large even in the central part of the hard alloy powder. The concentration of Co element shows lower but uniform distribution over the hard alloy powder, in which the concentration is lower in the hard alloy powder rather than in the outer side surrounding the hard alloy powder. This fact is considered to be due to the decreasing of particle number density of WC and the changing a hard Co bonding phase in the powder into the soft cast iron alloy layer. That is, the hardness gradually decrease in the bonding region shown in Fig. 5 is concluded to be due to the results mentioned above. As result of elution of Co element from the hard alloy powder causing by the heat of the molten iron, the interparticle spacing among WC particles increases to lead the decrease of the hardness in the hard alloy powder layer. As shown in Fig. 2, the thickness of inserted hard alloy layer was recognized to be thicker than the initial thickness before the casting. This fact is also understood to be due to the permeating of molten iron among WC particles in the hard alloy powder and leading the volume expansion of the hard alloy powder as mentioned above. This is supported by Fig. 7.

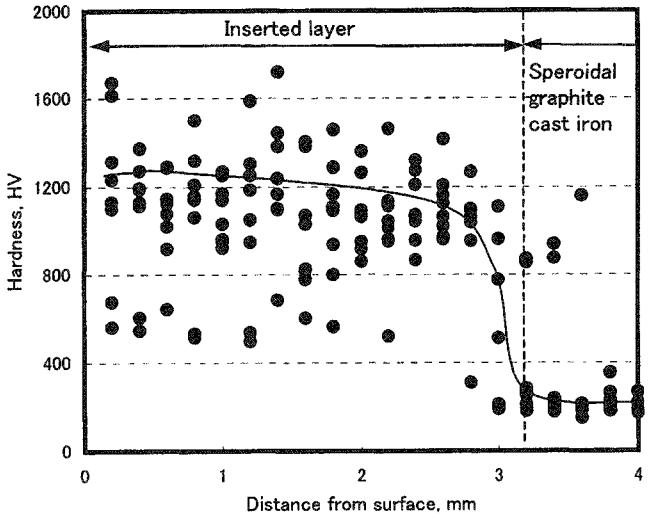

Figure 5 Relationship between microhardness and distance from the surface in the inserted specimen.

3. Hard facing of cast steel with hard alloy particles

3.1 Experimental method

The same self-curing mold as that in the case of cast iron was used as shown Fig. 1. The slurry of the hard alloy powder was pasted flat and smoothly by a thickness of 3mm onto the bottom of a test piece. In this case, a small amounts of nickel alloy powder (Ni-3.0mass%B-4.5mass%Si-0.06mass%C) and polyvinyl acetate were added to the hard alloy powder as a binder to make the slurry.

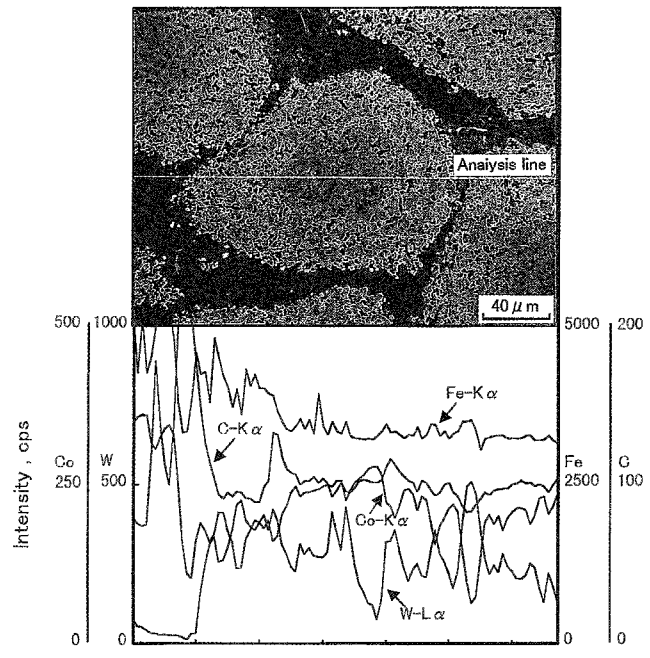

Figure 6 SEM image and EPMA line-analysis of a hard alloy powder showing HV1200 in the inserted layer.

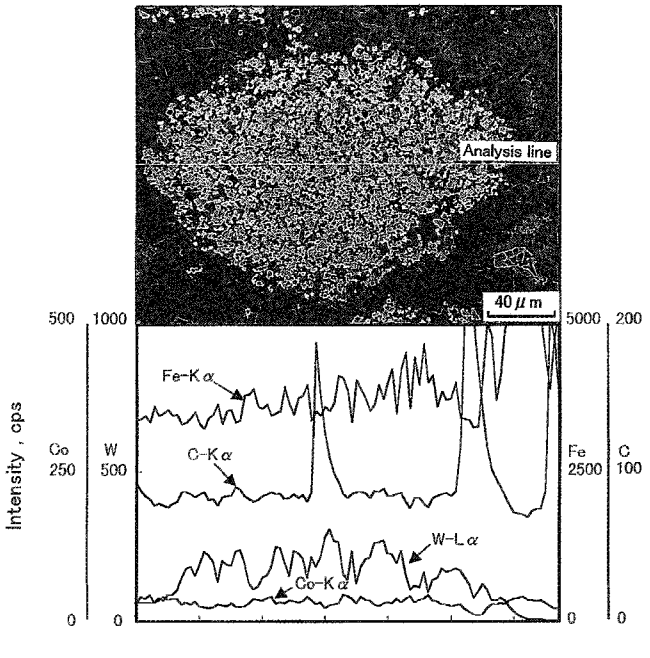

Figure 7 SEM image and EPMA line-analysis of a hard alloy powder showing HV600 in the inserted layer.

The base metal material used for the cast-in-insert was a low-alloy steel which was made from the melt blending a steel scrap, graphite powder, Fe-75mass%Si and Fe-60mass%Mn alloys as the raw materials.

For the melting, a high frequency induction furnace with a capacity of 100kg was used as well as the case of hard facing of the cast iron. Composition of the molten steel obtained was C : 0.29, Si : 0.43, Mn : 1.46, Cr : 0.050, S : 0.009 and P : 0.029mass%. After drying the slurry past layer, the molten steel was poured into the mold at the temperature of 1843K to make the test pieces.

3.2 Experimental Result and Discussion

3.2.1 Circumstance of Inserted Layer

In order to investigate the configuration of the inserted layer, the test piece was cut perpendicular to the bottom surface. The microstructure of the hard alloy layer on the cut surface was observed and shown in Fig. 8. Although the inserted alloy layer is recognized to be formed at the surface region of test piece, the morphology is not same as the case of the cast iron. As shown Fig. 8, the inserted layer appears to be a homogeneous layer of macrostructure, but still remaining the initial configuration of the particles. This is considered to be due to the liquid phase sintering during pouring. In this case, the pouring temperature is high enough to occur the liquid phase sintering because the temperature is above 1571K which is an eutectic temperature in W-C-Co system[2]

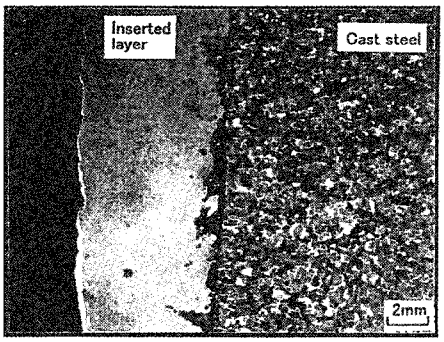

Figure 8 Macrostructure of the vertical cross-section in the inserted specimen. (In the case of locally hard faced cast steel.)

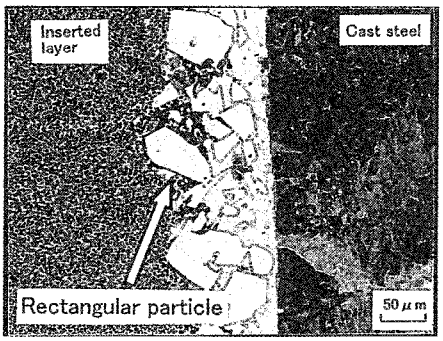

Figure 9 Microstructure of bonding region.

3.2.2 Structure of Inserted Layer

Figure 9 shows the microstructure of bonding region between the inserted layer and the base cast steel. A white intermediate layer containing many rectangular particles is recognized to be formed at the bonding region between the inserted layer and the base steel material. Moreover, Fig. 10 shows the distribution of each element in the neighborhood of a bonding region, which was obtained by EPMA. Fe element which is main element of cast steel is deeply permeating into the hard alloy layer, while Co element is distributing in the intermediate bonding region between the hard alloy layer and the cast steel layer. In the intermediate bonding region we can see many rectangular particles in which the X-ray intensities of W and Fe elements are detected strongly. In order to reveal further details on the microstructure of the intermediate region, the surface of the cast steel specimen was ground little by little to intermediate region to be observed the microstructure. The results obtained are shown in Fig. 11. Figure 11(a) shows the microstructure in the region of cast steel side, which shows the retained austenite containing martensite and banite phase.

Furthermore, Fig. 11(b) shows the microstructure in the middle region, which is constituted of the primary δ phase surrounded by

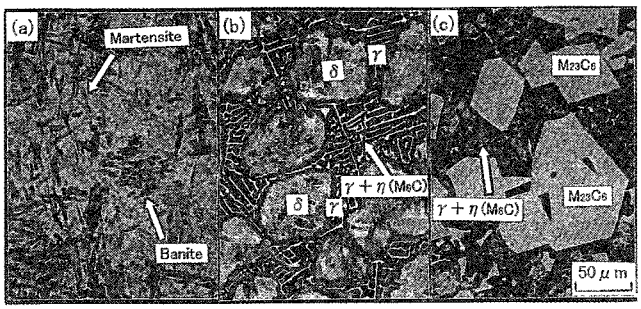

Figure 11 SEM cross-sectional image and EPMA in the insert specimen, which show (a) SEM image, (b) W map, (c) Co map and (d) Fe map, A and B show the inserted layer and cast steel, respectively.

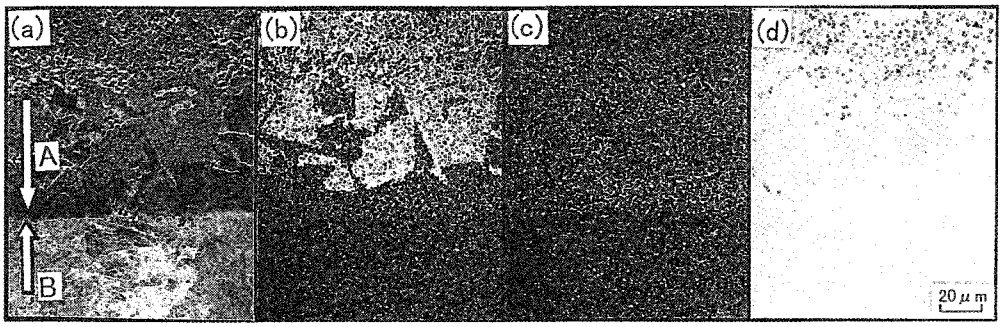

Figure 10 Microstructure of intermediate layer, which show (a) cast steel side, (b) middle and (c) hard alloy side.

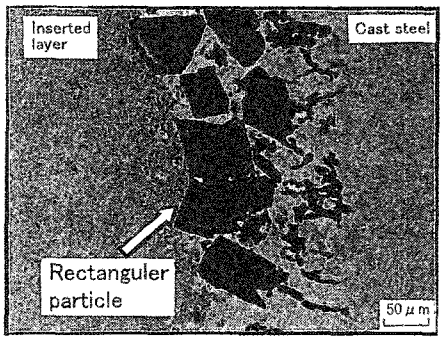

Figure 12 Microstructure of rectangular particle in the bonding region etched by potassium ferricyanide.

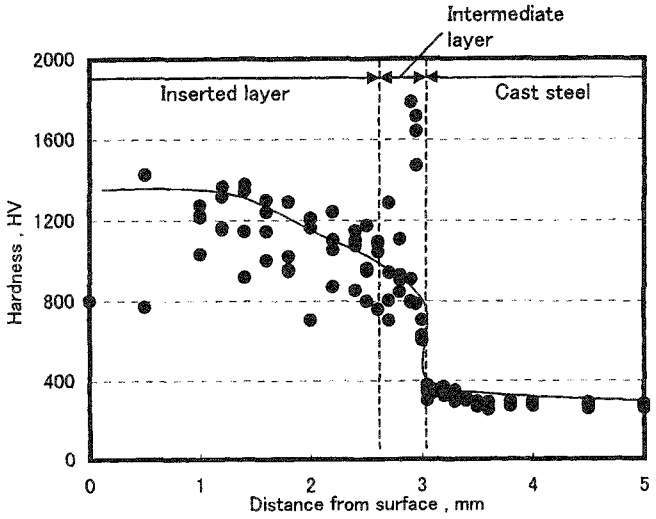

Figure 13 Relationship between microhardness and distance from the surface.

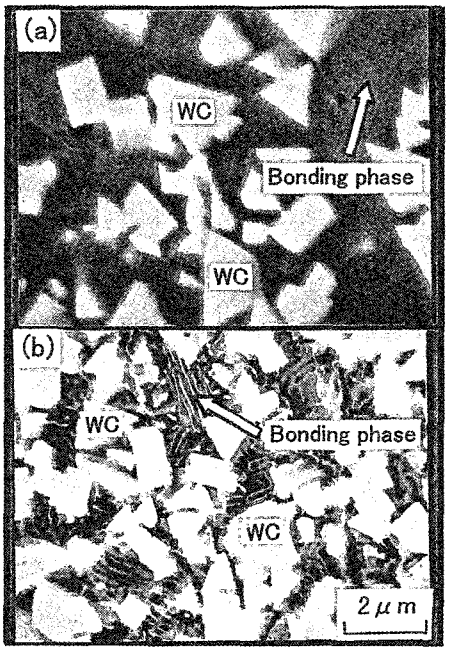

Figure 14 SEM image of inserted layer, which show (a) the region of HV1400 and (b) the region of HV800.

peritectic austenite phase and the eutectic phase of γ phase (austenite) + η phase (M_6C carbide). On the other hand, Fig. 11(c) shows the microstructure in the region of hard alloy side or inserted layer side, which is constituted of the primary $M_{23}C_6$ phase (rectangular phase) and the eutectic phase of γ phase (austenite) + η phase (M_6C carbide). The identification of these carbide phases was made by an etching method.

From the result obtained by EPMA, such the microstructures are considered to be caused by deeply diffusion of Co element into the cast steel layer.

Next, Fig. 12 shows the microstructure of the rectangular particles and W_6C eutectics which were etched with a reagent of potassium ferricyanide solution. The rectangular particles reacted vigorously with the reagent. Therefore, the rectangular particles are thought to be a complex carbide phases of $M_{23}C_6$ or M_6C. It is well known that many kinds of carbides such as $M_{23}C_6$ are formed in the W-C-Fe system phase diagram, while M_6C type carbide does not form in this system. In this experiment, however, Fe element of cast steel permeates into the hard alloy layer, while WC particles elute into the molten steel. Then, the intermediate layer is considered to form a structure of the W-C-Fe system. Therefore, the rectangular particles are considered to be $M_{23}C_6$ complex carbide.

3.2.3 Hardness of Inserted Layer

Figure 13 shows the hardness distribution in the inserted layer, which was measured by the micro Vickers hardness test (load ; 2.94N). The hardness values are distributing in a range from HV800 to HV1400. By the way, it is found that in the region of intermediate layer between the inserted layer and the cast steel (base metal) the hardness is decreasing gradually with increase in the distance from the surface in the same way as the case of the cast iron. Figure 14 shows the SEM images of the inserted layer. In the region corresponding to HV1400, the microstructure of bonding phase in the inserted layer shows austenite phase (γ phase) including hard martensite. On the other hand, in the region corresponding to HV800, the microstructure of bonding phase shows soft pearlite phase (the iron base matrix phase). This fact is considered to be due to the results of deep diffusion of Fe element into the central region of the inserted layer (hard alloy layer) from the cast steel side (base metal side) and also deep diffusion of Co elements into the intermediate layer from the inserted layer (hard alloy layer). Moreover, the peak hardness was observed in the intermediate layer. This peak value of HV1800 may be due to the complex carbide phase of $M_{23}C_6$.

4. Results

Applying the hard alloy powder on the surface of the mold for the cast-in-insert method, hard facing of spheroidal graphite cast iron and cast steel was conducted. The microstructure observation and the micro hardness test were conducted on the inserted layer of the test piece. The results obtained are as follows.

1. In the case of cast iron, the molten iron permeates among WC particles in the hard alloy powder. The WC particle in the inserted layer is enclosed by the molten iron. Therefore, the thickness of hard alloy layer becomes thicker than the initial thickness before the casting. The morphology of graphite particles in the cast iron among the hard alloy powder is flaky because of the reaction of the molten iron with W and Co elements which are eluted from the hard alloy powder.

2. The hardness in the inserted layer ranged from HV600 to HV1600, which is sufficiently high in comparison with HV200 in the cast iron base metal.
Therefore, the cast-in-insert method is very effective for the hard facing of spheroidal graphite cast iron.
3. The hardness in the bonding region between the inserted layer and the base cast iron layer gradually changes. This fact is considered to be due to the permeating of molten iron among WC particles to lead the volume expansion of the hard alloy powder. That is, the increasing interparticle spacing among WC particles leads the decrease of hardness.
4. In the case of cast steel, the configuration of the inserted layer shows a homogeneous layer, but still remaining the initial configuration of the particles. However, an intermediate layer containing rectangular particles is formed at the bonding region between the inserted layer and the base steel material. These rectangular particles were identified to be $M_{23}C_6$ type complex carbide.
5. The hardness in the inserted layer ranged from HV800 to HV1400. The hardness in the intermediate layer containing the complex carbides showed a peak hardness of HV1800.

References

[1] E. A. Brandes : Smithells Metals Reference Book, "Equilibr ium diagrams" Butterworth & Co Ltd, 6th Ed., (1983) 11-187, 11-263

[2] Rautala P. and Norton J. T. : J. Met. 10, P.1045 (1952)